AMERICAN JOURNAL OF RESEARCH IN MEDICAL SCIENCES, 2018
VOL 2, NO. 1: 24-33
10.5455/ajrms281645

eJManager

ORIGINAL ARTICLE

Open Access

Role of melatonin in ameliorating cytotoxic effect of gold nanoparticles on the pulmonary alveoli of adult albino rats

Ehab Mostafa Elzawawy, Abeer Gaber Ahmed

Department of Anatomy, Faculty of Medicine, Alexandria University, Egypt

ABSTRACT

Introduction: Environmental exposure to nanoparticles is inevitable as they became part of our daily life. Nanoparticles are widely distributed in air, cosmetics and medicines and even in food and as a result, nanotoxicity research is gaining attention. Gold nanoparticles (AuNPs) can cause lung damage through increased oxidative stress. Melatonin has a huge protective effect on all organs of the body through regulation of antioxidant enzymes.

Objective: In the present study we examined the possible histological alterations in the pulmonary alveoli after administration of 10 nm AuNPs in an attempt to understand the toxicity of AuNPs and the possible protective effect of concomitant administration of melatonin.

Material & methods: 30 healthy adult male albino rats were used. They were divided into 3 groups; control group (10 animals), AuNPs group: 10 animals treated with 4 mg/kg of 10 nm AuNPs once daily for 7 consecutive days and AuNPs+ melatonin group: 10 rats treated with 4 mg/kg of 10 nm AuNPs and 10 mg/kg melatonin at the same time once daily for 7 consecutive days.

Results: Exposure to AuNPs induced alterations in the pulmonary alveoli which were summarized mainly as destruction of type 1 and type 2 pneumocytes, thick interalveolar septa due to cellular infiltration. There was mild affection of pulmonary alveoli in the AuNPs+ melatonin group; few alveoli appeared slightly collapsed, separated by slightly thickened interalveolar septa due to mild cellular infiltration.

Conclusion: AuNPs induced evident damage in rat pulmonary alveoli. Melatonin significantly ameliorated the alveolar damage.

ARTICLE HISTORY

Received 16 July 2017
Accepted 12 October 2017
Published 22 October 2017

KEYWORDS

AuNPs; Melatonin; Pulmonary alveoli; Nanotoxicity; Oxidative stress

Introduction

Nanoparticles (NPs) have recently emerged as a promising field for the diagnosis and treatment of a variety of diseases [1]. Gold nanoparticles (AuNPs) are particularly promising because of their ease of synthesis in various sizes and shapes and the potential for conjugation with peptides and proteins, which can aim for specific targets. They can be used in various fields, including drug and gene delivery, cancer treatment and diagnostic tools [2].

Bulk gold is well known to be safe and chemically inert, and gold based compounds are used in many biological and biomedical applications. In spite of its beneficial outcomes in various fields, engineered AuNPs become highly active at nanometer dimensions and have created a worldwide concern due to their toxicities on human health [3].

Several studies [4,5] have shown that AuNPs can cause lung damage in the form of collapsed alveoli, destruction of type 1 pneumocytes, proliferation of type 2 pneumocytes and thick interalveolar septa due to cellular infiltration. This may be the result of AuNPs induced increases in oxidative stress and inflammation.

Contact Ehab Mostafa Elzawawy ehabzawawy@gmail.com Department of Anatomy, Faculty of Medicine, Alexandria University, Egypt

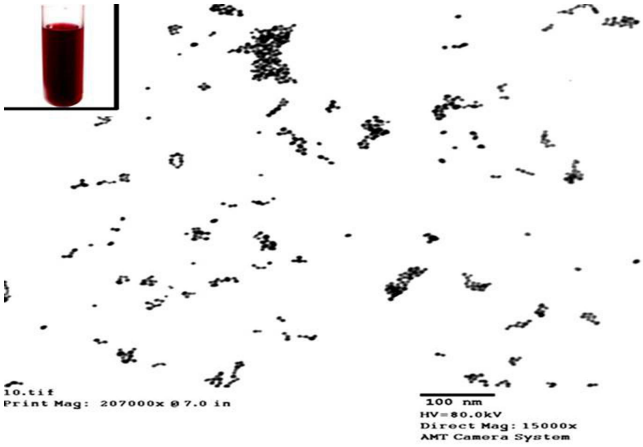

Fig 1. TEM micrograph of gold nanoparticles; spherical in shape and have a size range of 9.13-11.40 nm. (Print Mag. X207.000).

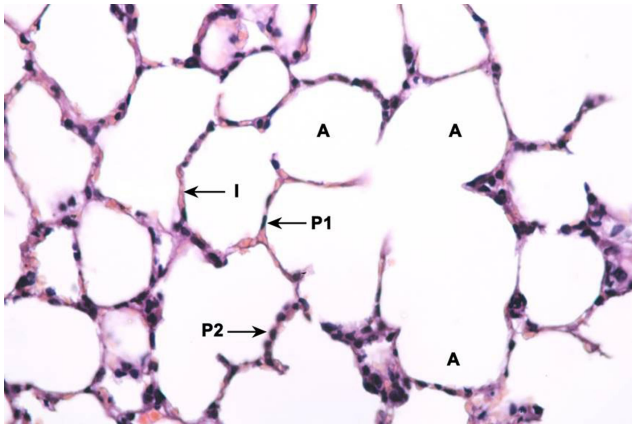

Fig 2. A photomicrograph of control rat lung (group I) showing normally distended pulmonary alveoli (A) separated by thin interalveolar septa (I). The alveoli are lined by flat type 1 pneumocytes (P1) and cuboid type 2 pneumocytes (P2) (H&E Stain, Mic. Mag X400).

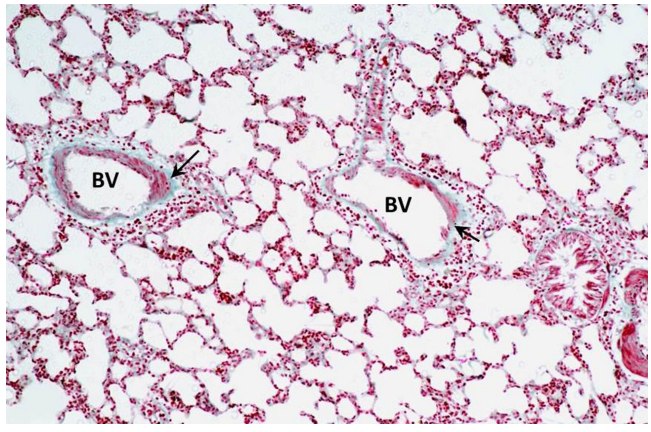

Fig 3. A photomicrograph of control rat lung (group I) showing normal amount and distribution of collagen fibers (↑) surrounding thin walled blood capillaries (BV) with normal size and shape (Gomori's Trichrome Stain, Mic. Mag X100).

Fig 4. Electron micrograph of control rat lung (group I) showing normal size and shape type 1 pneumoncyte (P1) having regular oval nucleus (N) with dense peripheral chromatin (Urinyl acetate, Lead citrate stain, Mic. Mag. X3000).

Increased oxidative stress leads to increased reactive oxygen species (ROS) production. ROS causes decreased mitochondrial membrane potential, impaired mitochondrial respiration, mitochondrial fragmentation and altered mitochondrial morphology [6].

Melatonin is a naturally occurring compound that has an antioxidant effect as it is a potent free radical recipient and can inhibit the formation of lipid peroxides, thus, guarding against oxidative stress [7].

Karaoz et al [8] studied the ameliorating effect of melatonin histologically and biochemically in lung tissues in rats exposed to chlorpyriphos-ethyl (CE). Melatonin considerably reduces CE toxicity in lung tissues of rats.

Objective

The objective of the present study was to investigate the effects of AuNPs on the pulmonary alveoli of rats in an attempt to understand their toxicity and find out the potential role of melatonin in ameliorating these toxic effects if any.

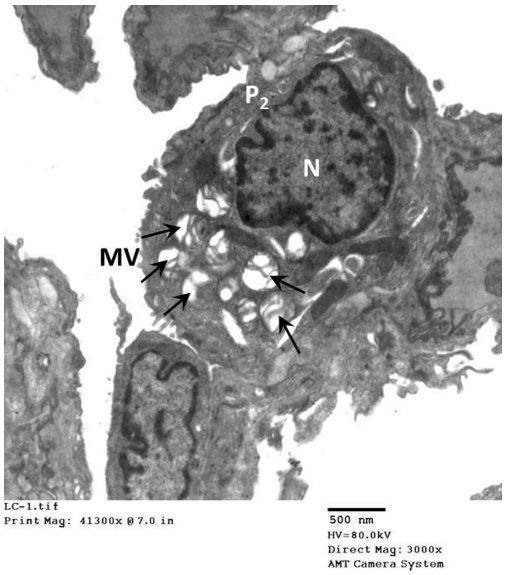

Fig 5. Electron micrograph of control rat lung (group I) showing normal size and shape type 2 pneumoncyte (P2) with regular nucleus (N) that has dense peripheral chromatin. The cell contains variable sized characteristic lamellar bodies filled with surfactant (↑) and has normal apical microvilli (MV) (Urinyl acetate, Lead citrate stain, Mic. Mag. X3000).

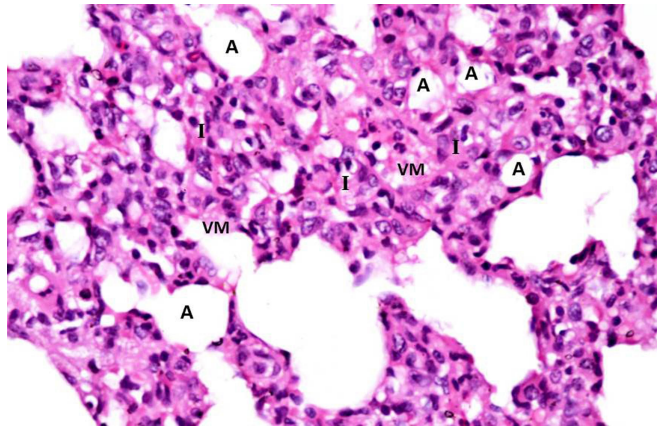

Fig 7. A photomicrograph of group II rat lung showing collapsed alveoli (A) separated by thick interalveolar septa (I) which contain foam macrophages (VM) filled with phospholipid vacuoles (H&E Stain, Mic. Mag X400).

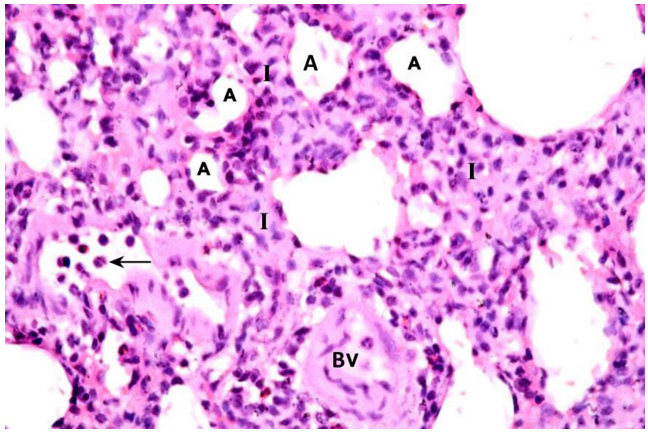

Fig 6. A photomicrograph of group II rat lung showing collapsed alveoli (A) separated by thick interalveolar septa (I) due to cellular infiltration and accumulation of acidophilic hyaline material. There are desquamated cells in the alveoli (↑). The blood capillaries (BV) are congested and filled with acidophilic hyaline material (H&E Stain, Mic. Mag X400).

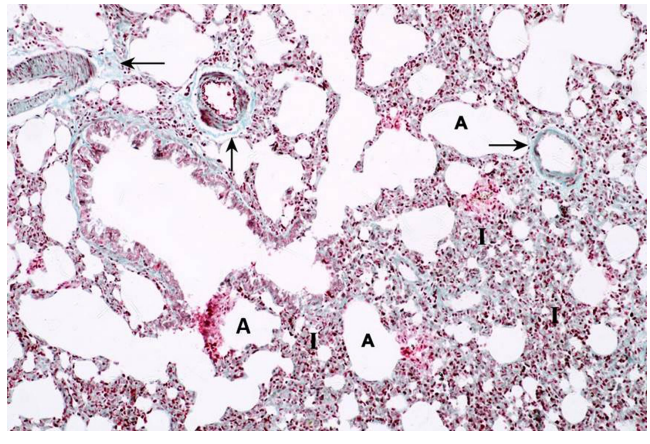

Fig 8. A photomicrograph of group II rat lung showing collapsed alveoli (A) and thick interalveolar septa (I). There is an increased amount and abnormal distribution of collagen fibers especially around blood capillaries (↑) (Gomori's Trichrome Stain, Mic. Mag X100).

Material

This study was carried out on 30 adult male albino rats, each of an average weight ranging from 150-200 gm, and of age about 3-4 months. The animals were maintained under standard laboratory conditions. Guidelines for care and use of animals, approved by the Animal House Center, Faculty of Medicine, University of Alexandria, were followed.

The animals were randomly divided into 3 groups:

Group I (control group)

10 rats were subdivided into two equal Subgroups, 5 animals each:

Subgroup Ia: (negative control) rats were injected intraperitoneally with 200 µl phosphate buffer saline for 7 days.

Subgroup Ib: (positive control) rats were injected intraperitoneally with 200 µl of 1% Trisodium citrate dihydrate for 7 days.

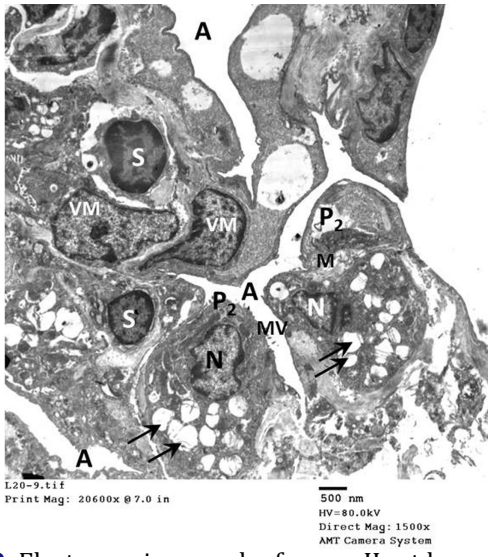

Fig 9. Electron micrograph of group II rat lung showing collapsed alveoli (A), numerous abnormal type 2 pneumoncytes (P2) that have shrunken irregular eccentric nuclei (N), few microvilli (MV), empty lamellar bodies with irregular outline (↑) and mitochondria with vacuolated matrix (M). The interalveolar septa are thickened by foamy vacuolated macrophages (VM) that have dense irregular nuclei and by septal cells (S) (Urinyl acetate, Lead citrate stain, Mic. Mag. X1500).

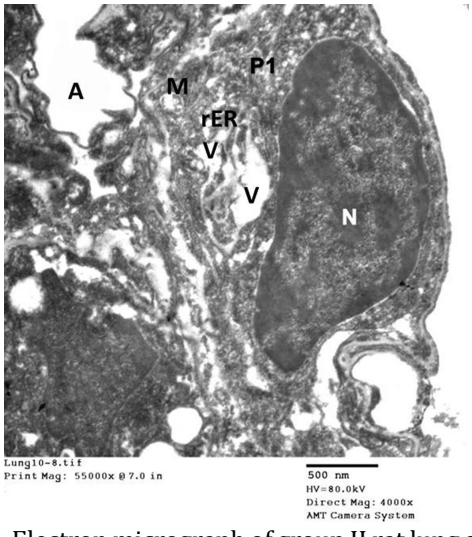

Fig 10. Electron micrograph of group II rat lung showing collapsed alveoli (A) lined by abnormal type 1 pneumocyte (P1) which has a large irregular pyknotic nucleus (N) that contains chromatin disappeared all over and not only peripherally, vacuolated cytoplasm (V), dilated rough endoplasmic reticulum (rEP) and degenerated mitochondria (M) with vacuolated matrix (Urinyl acetate, Lead citrate stain, Mic. Mag. X4000).

Group II (AuNPs group)

10 rats were treated with AuNPs of size10 nm. They received an intraperitoneal injection of 200 µl of AuNPs solution at a dose of 4 mg/kg once a day for 7 days, based on the previously identified toxic dose in vivo [4].

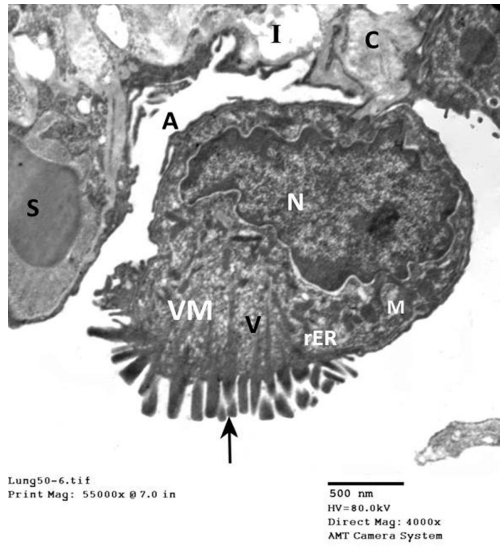

Fig 11. Electron micrograph of group II rat lung showing activated alveolar macrophage (VM) with hypertrophied lamellopodia (↑), irregular dark nucleus (N), vacuolated cytoplasm (v), dilated rough endoplasmic reticulum (rEP) and dense mitochondria (M). The interalveolar septum (I) contains collagen fibers (C) and inflammatory septal cells (S). Note: The alveoli (A) are collapsed (Urinyl acetate, Lead citrate stain, Mic. Mag. X4000).

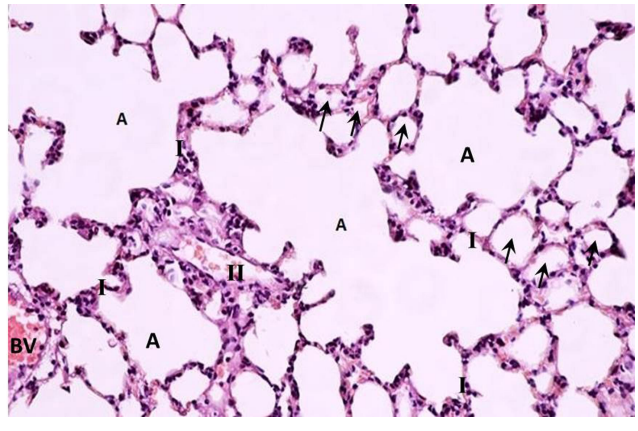

Fig 12. A photomicrograph of group III rat lung showing normally distended pulmonary alveoli (A). Few alveoli are collapsed (↑). The interalveolar septa are mainly thin (I) except in a few places where it is thickened by mild cellular infiltration (II). Blood capillaries (BV) have normal appearance (H&E Stain, Mic. Mag X400).

Group III (AuNPs+ melatonin group)

10 rats were treated with AuNPs of size10 nm and melatonin at the same time. They received an intraperitoneal injection of 200 µl of AuNPs solution at a dose of 4 mg/kg once a day for 7 days. They also received melatonin administered intramuscularly at a dose of 10 mg/kg once a day for 7 days, based on the previously identified protective dose in vivo [8].

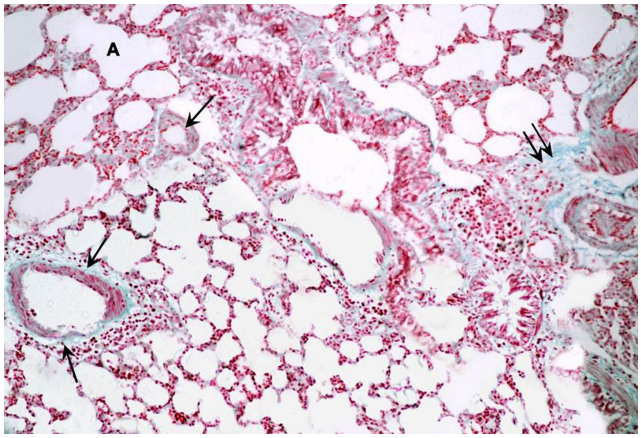

Fig 13. A photomicrograph of group III rat lung showing normal amount and distribution of collagen fibers (↑) except in a few places where it is slightly increased (↑ ↑). The alveoli (A) are normal (Gomori's Trichrome Stain, Mic. Mag X100).

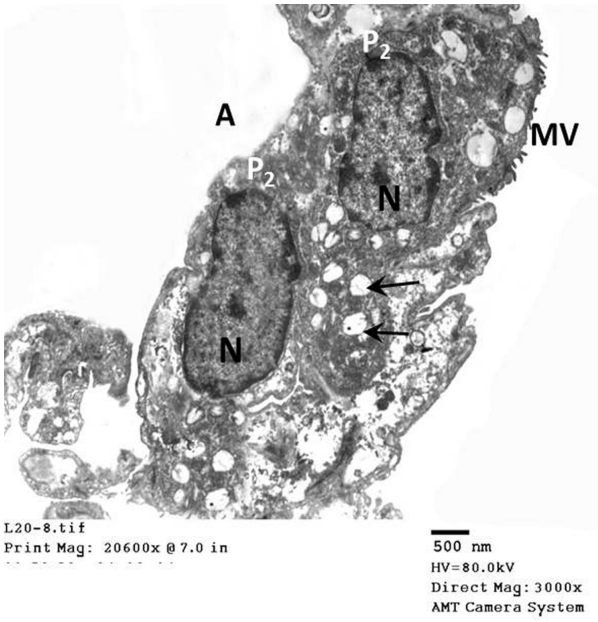

Fig 14. Electron micrograph of group III rat lung showing normal type 2 pneumocytes (P2) containing normal shape and size nuclei (N) with peripheral chromatin, normal lamellar bodies filled with surfactant (↑) and normal microvillous (MV) border. The alveoli (A) are normal in size (Urinyl acetate, Lead citrate stain, Mic. Mag. X3000).

Methods

(1) Preparation of gold nanoparticles (AuNPs)

The gold nanoparticles were prepared following the method introduced by Kimling et al [9]. A volume of 5 mL of 0.01% Tetrachloroauric acid solution is refluxed, and 200 µl of 1% Trisodium citrate dihydrate solution is added to the boiling solution. Reduction of gold ions by the citrate ions is completed after five minutes and the solution is further boiled for 30 minutes and then left to cool at room temperature. This method yields spherical particles with an average diameter of about 10nm. For control group Ia, phosphate buffer saline (PBS) solution was prepared.

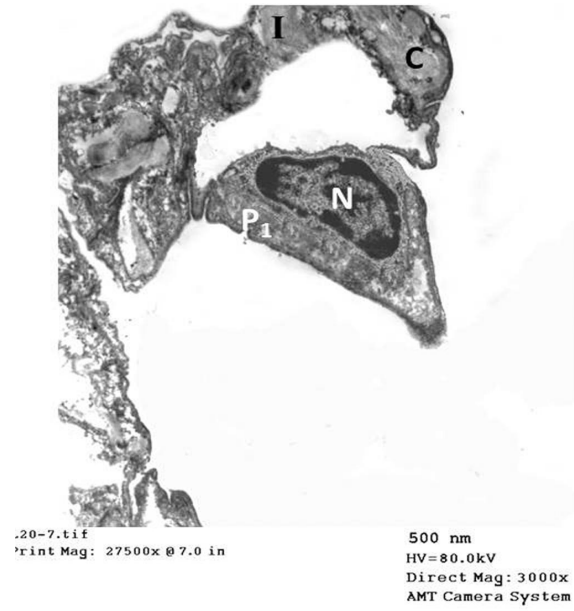

Fig 15. Electron micrograph of group III rat lung showing normal type 1 pneumocyte (P1) with a regular oval nucleus (N) with dense peripheral chromatin and normal clear cytoplasm, the interalveolar septum (I) is slightly thickened by few collagen fibers (C) (Urinyl acetate, Lead citrate stain, Mic. Mag. X3000.

(2) Characterization of the prepared AuNPs

The prepared AuNPs were characterized using transmission electron microscopy (TEM) (Jeol 100 CX, Tokyo, Japan), Electron Microscopy Unit, Faculty of Science, University of Alexandria [10]. It is an excellent tool for characterizing the size of nanoparticles. It can yield information about the size and morphology of nanoparticles. A small drop of the AuNPs solution was placed onto TEM grids coated with a thin carbon film and allowed to evaporate. Then digital pictures of several locations on the grid were taken. The prepared AuNPs were spherical in shape with a size range of 9.13-11.40 nm (Fig. 1).

(3) Histological study

After 24 hours of the last injection (the eighth day), animals were sacrificed under ether anaesthesia. The left lung was excised and cut into 2 specimens as follows:

1. The first specimen was fixed in 10% formal saline and processed to get 6 µm thick paraffin sections. The histological sections were

stained with Haematoxylin and Eosin (H&E) stain and Gomori's Trichrome stain [11].
2. The second specimen was cut into small pieces (1/2-1 mm) and immediately fixed in 3% glutaraldehyde solution and processed to get ultrathin sections stained with Urinyl acetate, Lead citrate stain for electron microscopic examination [12].

Results

(I) Group I (control group)

1. Light microscopic results

a. Hematoxylin & eosin stain: Light microscopic examination of the histological sections of both negative and positive control subgroups revealed normal architecture of the pulmonary alveoli as evident by distended alveoli separated by thin interalveolar septa. The alveoli were lined by thin flat type 1 pneumocytes and few cuboidal type 2 pneumocytes that appeared bulging into the alveolar lumen (Fig. 2).

b. Gomori's trichrome stain: Light microscopic examination of the histological sections of both negative and positive control subgroups revealed normal architecture of pulmonary alveoli with normal amount and distribution of collagen fibres. Thin walled capillaries were seen ramifying in between the alveoli (Fig. 3).

2. Ultrastructural results

Electron microscopic examination of rat lungs of both negative and positive control subgroups showed the classical architecture of pulmonary alveoli with distended thin wall lined by type 1 pneumocytes having regular oval nucleus with dense peripheral chromatin and clear cytoplasm and type 2 pneumocytes with regular nucleus, apical microvilli facing alveolar lumen and contain variable sized characteristic lamellar bodies filled with surfactant (Figs. 4,5).

Group II (AuNPs group)

1. Light microscopic results

a. Hematoxylin & eosin stain: The following histological alterations were detected in the pulmonary alveoli of AuNPs treated rats. The alveoli were collapsed and separated by very thick interalveolar septa due to cellular infiltration with foamy macrophages due to accumulation of phospholipid vacuoles inside the cells (foam cells) and presence of phospholipids in the septa as an acidophilic hyaline material. The alveoli contained some desquamated cells and blood capillaries were congested and filled with acidophilic hyaline material (Figs. 6,7).

b. Gomori's trichrome stain: The following histological alterations were detected in the pulmo nary alveoli of AuNP treated rat lungs; collapsed pulmonary alveoli, thick interalveolar septa and increased amount and abnormal distribution of colla- gen fibers especially around blood capillaries (Fig. 8).

2. Ultrastructural results

The following ultrastructural changes were detected in the pulmonary alveoli of AuNP treated rats: collapsed alveoli lined by abnormal type 1 pneumocytes with large irregular pyknotic nucleus (N) that contains chromatin disappeared all over and not only peripherally, vacuolated cytoplasm (V), dilated rough endoplasmic reticulum (rEP) and degenerated mitochondria (M) with vacuolated matrix. Type 2 pneumocytes were increased in number; they had shrunken irregular eccentric nuclei, empty lamellar bodies with irregular outline and scanty microvilli. The alveoli were separated by thick interalveolar septa due to cellular infiltration by different cells; mononuclear inflammatory cells (septal cells) and foamy vacuolated macrophages. Few macrophages were highly activated and were inside the alveoli. They had hypertrophied lamellopodia, irregular dark nuclei, vacuolated cytoplasm, dilated rough endoplasmic reticulum and dense mitochondria. There were large amount of collagen fibres deposited in the interalveolar septa (Figs. 9,10,11).

Group III (AuNPs+melatonin group)

1. Light microscopic results

a. Hematoxylin & eosin stain: The histological sections of rat lungs of group III revealed mild affection of pulmonary alveoli; few appeared slightly collapsed, separated by slightly thickened interalveolar septa due to mild mononuclear cellular infiltration. The majority of alveoli were normally distended. There were no desquamated cells in the alveoli. Blood capillaries had normal appearance. There was no acidophilic hyaline material in interalveolar septa or blood capillaries (Fig. 12).

b. Gomori's trichrome stain: The histological sections of rat lungs of group III revealed normal alveoli and blood capillaries and normal amount and distribution of collagen fibers except in a few places where it was slightly increased (Fig. 13).

2. Ultrastructural results

Electron microscopic examination of rat lung of group III revealed less affected pulmonary alveoli; only few of them were collapsed, type1 and type 2 pneumocytes had normal nuclei and cell organelles. The interalveolar septa in a few places were slightly thickened by few collagen fibers. There were no activated macrophages. (Figs. 14,15).

Discussion

Unique physicochemical properties of engineered nanoparticles, which are responsible for the beneficial outcome, are also responsible for its toxicities. AuNPs are one of the leading nanoparticles currently under investigation due to their applicability in various fields [3].

Nanotoxicological studies are intended to determine whether and to what extent these properties may pose a threat to the environment and to human beings. The mechanism of nanoparticles toxicity may be due to generation of free radicals and presence of transition metals [13].

The potential for biological injury lies in the novel physicochemical properties of NPs as they approach the sub-100 nm length scale. NPs have a much larger surface area to volume ratio than do bulk materials, which means that an increased number of atoms are exposed at the material's surface. The interactions taking place at the nano-bio interface could have many consequences including membrane permeability changes, gene mutations, signaling effects, ionic exchanges, biocatalytic changes, enzyme failure and ultimately inducing apoptosis [3,14].

The ability of AuNPs to generate oxidative stress has formed the basis of their hypothetical toxicity [15,16].

The mechanism of alveolar inflammation that follows NPs deposition is caused by Redox-sensitive transcription factors, such as NF-kB (nuclear factor kappa-light-chain-enhancer of activated B cells). When these transcription factors are activated, they lead to the transcription of proinflammatory genes, which in turn lead to the production of cytokines, chemokines, and adhesion molecules [17].

Previous studies [4,18] as well as our own have shown that AuNPs pass through the alveolar–capillary barrier. Therefore, inhaled NPs can penetrate into blood circulation and NPs in the blood stream can reach lung alveoli.

In the present study, evident histological alterations in the pulmonary alveoli were induced by administration of AuNPs. This is in agreement with the data obtained from previous studies; Johnston et al [14] and Abdelhalim et al [15].

These changes included collapsed alveoli due to deficient surfactant, destruction of type1 and type2 pneumocytes and degenerated organelles. The interalveolar septa were greatly thickened due to cellular infiltration, presence of acidophilic hyaline material and increased collagen fibers. Macrophages were lodged in the interalveolar septa and also inside the pulmonary alveoli. Blood capillaries were congested and filled with acidophilic hyaline material due to destruction of type2 pneumocytes and extrusion of surfactant present in their lamellar bodies. These cells had scanty microvilli denoting inability to secrete surfactant.

Sadauskas et al [18] described hypertrophy of type2 pneumocytes in AuNPs treated rats with distended lamellar bodies filled with surfactant. They considered type2 Pneumocytes hyperplasia as an early response to alveolar injury. They assumed that cellular hyperplasia occurred as a regenerative trial to replace the damaged alveolar cells. It is known that type2 pneumocytes are the progenitors of type1 cells. The increased number of type2 pneumocytes observed in the present study may be due to delayed differentiation into type1 pneumocytes.

Also, inflammatory process caused by nanotoxicity may induce conversion of bone marrow mesenchymal stem cells into type2 pneumocytes leading to increase their number. The lamellar bodies in the beginning of nanotoxicity are filled with surfactant due to increased production or reabsorption by type2 pneumocytes. Later on, accumulation of surfactant in foam macrophages which was also observed in the present study means extrusion from lamellar bodies due to destruction of type2 pneumocytes [18].

The present study proved that AuNPs can exert damaging effect on type2 pneumocytes leading to surfactant deficiency. Intracellular surfactant deficiency causes adult respiratory distress syndrome (ARDS) because pulmonary surfactant is crucial in the prevention of alveolar collapse by reducing alveolar surface tension [16].

Extravascular localization of leukocytes implies acute vascular endothelial injury which is a consistent feature of injury caused by most pulmonary toxicants. The infiltrating inflammatory cells account for damaging the alveolar and interstitial pulmonary structures through the lytic effect of their enzymes [19].

Additionally, AuNPs may induce or aggravate inflammatory and allergic responses by directly influencing immune-related cell populations in the lung. After lung exposure, NPs recruit granulocytes to the lung, and some end up in alveolar macrophages. Also, surfactant is incorporated in the lung host defense mechanism through augmentation of alveolar macrophage migration [20].

Activated alveolar macrophages that have hypertrophied lamellopodia and filled with vacuolated material were noted in our specimen. They amplify and accentuate the primary lesions through elaboration of inflammatory chemotactic cytokines. These changes are commonly described with severe lung injury and inflammatory lung diseases [15,16].

The results of the present study agree with previous reports of Morimoto et al [20], Gelli et al [21] and Liu et al [22]. They reported that NPs produce pulmonary toxicity through increased oxidative stress and persistent inflammation.

The present study showed increased deposition of collagen fibers in the interalveolar septa. This was possibly initiated by the local hypoxia created at the damaged tissue and reflects activation of inflammatory mononuclear (septal) cells due to the effect of mitogenic factors released from activated macrophages. Pulmonary fibrosis is a common pathologic feature observed after exposure to NPs [19].

Kim et al [23] reported that copper nanoparticle exposure induce inflammatory responses with increased recruitment of inflammatory cells especially macrophages in the lungs leading to pulmonary fibrosis. They concluded that persistent oxidative stress and inflammation in lungs after exposure to NPs are thought to be the underlying cause for lung fibrosis.

Enhancement of antioxidant enzymes of alveolar macrophages was demonstrated after in vivo exposure to Copper NPs. However, this was not sufficient to counteract the lipid peroxidation and hydrogen peroxide generation that occurred. Thus, the overall resultant effect was induction of oxidative stress in the cells [24].

Melatonin can oppose the oxidative stress in mitochondria and the NPs induced-inhibition of ATP by increasing ATP synthesis [25]. It is called the suicidal antioxidant, as it is consumed during its action. That's why intense oxidative stress results in an acute decrease in circulating melatonin levels [26]. During the recent disaster in Japan, melatonin was used to prevent the damage induced by ionizing radiation [27].

Melatonin exerts its effects through activation of at least two high-affinity G-protein-coupled receptors, MT1 and MT2. Effector systems involved in MT1and MT2 melatonin receptor signaling through G-protein coupling include adenylyl cyclase, phospholipase C, phospholipase A2, potassium channels and calcium channels [28].

Taslidere et al [29] suggested that agents with antioxidant properties such as melatonin and quercetin may have positive effects in the prevention of pulmonary diseases characterized especially by inflammation, and fibrosis.

Puiq et al [30] and Zhou et al [31] concluded that melatonin treatment was able to modulate the inflammatory and apoptosis status of the lung due to age-induced damage or ischemic insult through inhibition of NF-kB signaling pathways.

In the present study, addition of melatonin had a great protective value, type1 and type2 pneumocytes had normal shape, size and organelles. The blood capillaries were normal; there was no endothelial injury or acidophilic hyaline material. However, there were mild mononuclear cellular infiltration and slightly increased collagen fibers in the interalveolar septa indicating mild inflammation. There were no activated alveolar macrophages.

Pohlmann et al [32] demonstrated a huge increase of the antioxidant effect of melatonin when used in NPs and they suggested the use of this form of melatonin to counteract oxidative stress caused by other NPs.

Charão et al [33] found out that melatonin lipid-core nanocapsules have a great protective antioxidant property. They efficiently protect pneumocytes against the cytotoxic and genotoxic effects of paraquat.

Komninou et al [34] have indicated that melatonin lipid-core nanocapsules increase the protective effects of melatonin against oxidative stress and cell apoptosis during in vitro embryo culture in bovine species.

Remião et al [35] concluded that when melatonin lipid-core nanocapsules were applied during in vitro oocyte maturation in humans; ROS levels and apoptotic cell number/blastocyst ratio were decreased, while cleavage and blastocyst rates were increased.

D'Almeida et al [36] confirmed that α-bis- lipid-core nanocapsules significantly reduced airway hyperreactivity, neutrophil infiltration, chemokine levels and tissue lung injury 18 hours after the liposaccharide challenge. They were able to prevent ARDS in mice.

AuNPs have a damaging effect on the lung alveoli; melatonin has a partial protective effect. Concomitant use of other antioxidant with melatonin could have a complete protective value. Also, the use of melatonin as NPs may have a greater protective value against the toxicity of other NPs.

Conflicts of Interest

The authors declare that there are no conflicts of interest.

References

[1] Hughes GA. Nanostructure-mediated drug delivery. Nanomedicine 2005; 1(1):22-30.

[2] Huang X, El-Sayed M. Gold nanoparticles: optical properties and implementations in cancer diagnosis and photothermal therapy. Journal of Advanced Research 2010; 1(1):13-28.

[3] Daniel MC, Astruc D. Gold nanoparticles: Assembly, supramolecular chemistry, quantum - size- related properties and applications toward biology, catalysis and nanotechnology. Chem Rev 2004; 104(1):293-346.

[4] Zhang XD, Wu HY, Wu D, Wang YY, Chang JH, Zhai ZB, Meng AM, Liu PX, Zhang LA, Fan FY. Toxicologic effects of gold nanoparticles in vivo by different administration routes. Int J Nanomedicine. 2010; 5:771-81.

[5] Jia HY, Liu Y, Zhang XJ, Han L, Du LB, Tian Q, Xu YC. Potential oxidative stress of gold nanoparticles by induced -NO releasing in serum. J Am Chem Soc 2009; 131(1):40-41.

[6] Madl AK, Plummer LE, Carosino C, Pinkerton KE. Nanoparticles, lung injury, and the role of oxidant stress. Annu Rev Physiol 2014; 76:447-65.

[7] Rodriguez C, Mayo JC, Sainz RM, Antolín I, Herrera F, Martín V, Reiter RJ. Regulation of antioxidant enzymes: a significant role for melatonin. J Pineal Res 2004; 36(1):1–9.

[8] Karaoz E, Gultekin F, Akdogan M, Oncu M, Gokcimen A. Protective role of melatonin and a combination of vitamin C and vitamin E on lung toxicity induced by chlorpyrifos-ethyl in rats. Exp Toxicol Path 2002; 54(2)97-108.

[9] Kimling J, Maier M, Okenve B, Kotaidis V, Ballot H, Plech A. Turkevich method for gold nanoparticle synthesis revisited. J Phys Chem B 2006; 110(32):15700–15707.

[10] Dykman LA, Bogatyrev VA. Gold nanoparticles: preparation, functionalisation and applications in biochemistry and immunochemistry. Russ Chem Rev 2007; 76:181-94.

[11] Bancroft JD, Gamble M. Theory and practice of histological techniques. 6th ed: Elsevier Health Sciences; 2008.

[12] Kuo J. Electron microscopy: methods and protocols. 2nd ed: Springer; 2007.

[13] Pan Y, Leifert A, Ruau D, Neuss S, Bornemann J, Schmid G, Brandau W, Simon U, Jahnen-Dechent W. Gold nanoparticles of diameter 1.4 nm trigger necrosis by oxidative stress and mitochondrial damage. Small 2009; 5(18):2067-2076.

[14] Johnston HJ, Hutchison G, Christensen FM, Peters S, Hankin S, Stone V. A review of the in vivo and in vitro toxicity of silver and gold particulates: Particle attributes and biological mechanisms responsible for the observed toxicity. Crit Rev Toxicol 2010; 40(4):328-46.

[15] Abdelhalim MAK. Exposure to gold nanoparticles produces pneumonia, fibrosis, chronic inflammatory cell infiltrates, congested and dilated blood vessels, and hemosidrin granule and emphysema. J Cancer Sci Ther 2012; 4(3):046-050.

[16] Schlinkert P, Casals E, Boyles M, Tischler U, Hornig E, Tran N, Zhao J, Himly M, Riediker M, Oostingh GJ, Puntes V, Duschl. The oxidative potential of differently charged silver and gold nanoparticles on three human lung epithelial cell types. J Nanobiotechnology 2015;13:1.

[17] Hussain S, Garantziotis S, Rodrigues-Lima F, Dupret JM, Baeza-Squiban A, Boland S. Intracellular Signal Modulation by Nanomaterials. Adv Exp Med Biol 2014; 811:111-134.

[18] Sadauskas E, Jacobsen NR, Danscher G,Stoltenberg M, Vogel U, Larsen A, Kreyling W, Wallin H. Biodistribution of gold nanoparticles in mouse lung following intratracheal instillation. Chem Cent J 2009; 3:16.

[19] Takenaka S, Möller W, Semmler-Behnke M, Karg EW, Wenk A, Schmid O, Stöger T, Jennen L, Aichler M, Walch AK, Pokhrel S, Mädler L, Eickelberg O, Kreyling WG..Efficient internalization and intracellular translocation of inhaled gold nanoparticles in rat alveolar macrophages. Nanomedicine 2012; 7(6):855-865.

[20] Morimoto Y, Izumi H, Kuroda E. Significance of Persistent Inflammation in Respiratory Disorders Induced by Nanoparticles. J Immunol Res 2014; ID 962871, 8.

[21] Gelli K, Porika M, Reddy AR. Assessment of pulmonary toxicity of MgO nanopar- ticles in rats. Environm Toxicol 2015; 30(3):308-314.

[22] Liu R, Yin L, Pu Y, Liang G, Zhang J, Su Y, Xiao z, Ye B. Pulmonary toxicity induced by three forms of titanium dioxide nanoparticles via intra-tracheal instillation in rats. Prog Nat Sci 2009; 19 (5):573–579.

[23] Kim J S, Adamacakova-Dodd A, Oshaughnessy P, Grassian V. Effects of copper nanoparticle exposure on host defense in a murine pulmonary infection model. Particle Fibre Toxicol 2011; 8 (10):8-29.

[24] Rani VS, Kumar AK, Kumar CP, Reddy AR. Pulmonary Toxicity of Copper Oxide (CuO) Nanoparticles in Rats. J Med Sci 2013; 13(7):571-577.

[25] Dragicevic N, Copes N, O'Neal-Moffitt G, Jin J, Buzzeo R, Mamcarz M, Tan J, Cao C, Olcese JM, Arendash GW, Bradshaw PC. Melatonin treatment restores mitochondrial function in Alzheimer's mice: a mitochondrial protective role of melatonin membrane receptor signaling. J Pineal Res 2011; 51,(1):75–86.

[26] Galano A, Tan DX, Reiter RJ. Melatonin as a natural ally against oxidative stress: a physicochemical examination. J Pineal Res. 2011; 51(1):1-16.

[27] Reiter RJ, Tan DX, Korkmaz A., Manchester LC. The disaster in Japan: utility of melatonin in providing protection against ionizing radiation. J Pineal Res 2011; 50:357–358.

[28] Dubocovich ML, Delagrange P, Krause DN, Sugden D, Cardinali DP, Olcese J. International union of basic and clinical pharmacology. LXXV. Nomenclature, classification, and pharmacology of G protein-coupled melatonin receptors. Pharmacol Rev 2010; 62(3):343–380.

[29] Taslidere E, Esrefoglu M, Elbe H, Cetin A, Ates B. Protective effects of melatonin and quercetin on experimental lung injury induced by carbon tetrachloride in rats. Exp Lung Res 2014; 40(2):59-65.

[30] Puig Á, Rancan L, Paredes SD, Carrasco A, Escames G, Vara E, Tresguerres JA. Melatonin decreases the expression of inflammation and apoptosis markers in the lung of a senescence-accelerated mice model. Exp Gerontol 2016; 75:1-7.

[31] Zhou L, Zhao D, An H, Zhang H, Jiang C, Yang B. Melatonin prevents lung injury induced by hepatic ischemia-reperfusion through anti-inflammatory and anti-apoptosis effects. Int Immunopharmacol 2015; 29(2):462-7.

[32] Pohlmann AR, Schaffazick SR, Creczynski-Pasa TB, Guterres SS. Preparation of drug-loaded polymeric nanoparticles and evaluation of the antioxidant activity against lipid peroxidation. Methods Mol Biol 2010; 610:109-21.

[33] Charão MF, Baierle M, Gauer B, Goethel G, Fracasso R, Paese K, Brucker N. Protective effects of melatonin-loaded lipid-core nanocapsules on paraquat-induced cytotoxicity and genotoxicity in a pulmonary cell line. Mutat Res Genet Toxicol Environ Mutagen 2015; 784-785:1-9.

[34] Komninou ER, Remião MH, Lucas CG, Domingues WB, Basso AC, Jornada DS, Deschamps JC. Effects of two types of melatonin-loaded nanocapsules with distinct supramolecular structures: polymeric (NC) and lipid-core nanocapsules (LNC) on bovine embryo culture model. PLOS one 2016; 11(6) e0157561.

[35] Remião MH, Lucas CG, Domingues WB, Silveira T, Barther NN, Komninou ER, Basso AC. Melatonin delivery by nanocapsules during in vitro bovine oocyte maturation decreased the reactive oxygen species of oocytes and embryos. Reprod Toxicol 2016; 63:70-81.

[36] D'Almeida APL, Pacheco de Oliveira MT, de Souza ÉT, de Sá Coutinho D, Ciambarella BT, Gomes CR, Terroso T, Guterres SS. α-bisabolol-loaded lipid-core nanocapsules reduce lipopolysaccharide-induced pulmonary inflammation in mice. Int J Nanomedicine. 2017;12:4479-4491.